



**CURRENT
PROTOCOLS**
A Wiley Brand

**Help move science
forward**

Our editors are looking for the best laboratory protocols that will yield reproducible results and are robust enough to be used by early career scientific researchers.

Our published laboratory protocols are highly detailed and annotated and ensure that researchers understand the factors critical for experimental success.

We welcome proposals from prospective authors for protocols or overviews that could fit the scope of our journal and meet the needs of our readers.



**Submit a
protocol
proposal**

 **Connect with us on Twitter @Curr_Protocols**

Software Tool for Automatic Quantification of Sarcomere Length and Organization in Fixed and Live 2D and 3D Muscle Cell Cultures *In Vitro*

Jeroen M. Stein,¹ Ulgu Arslan,¹ Marnix Franken,² Jessica C. de Greef,² Sian E. Harding,³ Neda Mohammadi,³ Valeria V. Orlova,¹ Milena Bellin,^{1,4,5} Christine L. Mummery,^{1,6,7} and Berend J. van Meer^{1,7,8}

¹Department of Anatomy and Embryology, Leiden University Medical Center, Leiden, The Netherlands

²Department of Human Genetics, Leiden University Medical Center, Leiden, The Netherlands

³National Heart and Lung Institute, Imperial College, London, United Kingdom

⁴Department of Biology, University of Padua, Padua, Italy

⁵Veneto Institute of Molecular Medicine, Padua, Italy

⁶Department of Applied Stem Cell Technologies, University of Twente, Enschede, The Netherlands

⁷These authors contributed equally to this work.

⁸Corresponding author: b.j.vanmeer@lumc.nl

Published in the Human Genetics section

Sarcomeres are the structural units of the contractile apparatus in cardiac and skeletal muscle cells. Changes in sarcomere characteristics are indicative of changes in the sarcomeric proteins and function during development and disease. Assessment of sarcomere length, alignment, and organization provides insight into disease and drug responses in striated muscle cells and models, ranging from cardiomyocytes and skeletal muscle cells derived from human pluripotent stem cells to adult muscle cells isolated from animals or humans. However, quantification of sarcomere length is typically time consuming and prone to user-specific selection bias. Automated analysis pipelines exist but these often require either specialized software or programming experience. In addition, these pipelines are often designed for only one type of cell model *in vitro*. Here, we present an easy-to-implement protocol and software tool for automated sarcomere length and organization quantification in a variety of striated muscle *in vitro* models: Two dimensional (2D) cardiomyocytes, three dimensional (3D) cardiac microtissues, isolated adult cardiomyocytes, and 3D tissue engineered skeletal muscles. Based on an existing mathematical algorithm, this image analysis software (SotaTool) automatically detects the direction in which the sarcomere organization is highest over the entire image and outputs the length and organization of sarcomeres. We also analyzed videos of live cells during contraction, thereby allowing measurement of contraction parameters like fractional shortening, contraction time, relaxation time, and beating frequency. In this protocol, we give a step-by-step guide on how to prepare, image, and automatically quantify sarcomere and contraction characteristics in different types of *in vitro* models and we provide basic validation and discussion of the limitations of the software tool. © 2022 The Authors. Current Protocols published by Wiley Periodicals LLC.

Basic Protocol: Staining and analyzing static hiPSC-CMs with SotaTool

Alternate Protocol: Sample preparation, acquisition, and quantification of fractional shortening in live reporter hiPSC lines

Support Protocol 1: Finding the image resolution

Support Protocol 2: Advanced analysis settings

Support Protocol 3: Finding sarcomere length in non-aligned cells

Keywords: cardiomyocytes • sarcomere length • sarcomere organization • skeletal muscle • software tool • stem cells

How to cite this article:

Stein, J. M., Arslan, U., Franken, M., de Greef, J. C., Harding, S. E., Mohammadi, N., Orlova, V. V., Bellin, M., Mummery, C. L., & van Meer, B. J. (2022). Software tool for automatic quantification of sarcomere length and organization in fixed and live 2D and 3D muscle cell cultures *in vitro*. *Current Protocols*, 2, e462. doi: 10.1002/cpz1.462

INTRODUCTION

Healthy adult muscle tissue is characteristic of striated sarcomeres (the contractile machinery) which are aligned and well organized along the length of each cell and the tissue axis. However, in conditions such as toxicity, disease, and during development, sarcomeres are less organized and achieve a decreased contraction force (Ribeiro et al., 2015). Cardiomyocytes and skeletal muscle cells can now be derived routinely and with high efficiency from human induced pluripotent stem cells (hiPSCs) using a variety of protocols based on defined culture media and differentiation factors (Birket et al., 2015; Mills et al., 2017). However, hiPSC-derived cardiomyocytes (hiPSC-CMs) and hiPSC-derived skeletal muscle (hiPSC-SM) are often structurally and functionally immature which is why the induction of maturation via new methods is widely studied (Jalal, Dastidar, & Tedesco, 2021; Yang, Pabon, & Murry, 2014). This immaturity and contractile deficiency are associated with a reduced sarcomere length, which is $\sim 2.2 \mu\text{m}$ in adult human cardiomyocytes but usually around $\sim 1.65 \mu\text{m}$ in immature hiPSC-CMs (Cohn et al., 2019; Gerbin et al., 2021; Giacomelli et al., 2020; van der Velden et al., 1998). Similarly, many cardiac genetic diseases, such as hypertrophic cardiomyopathy, which is caused by mutations in myosin heavy chain or myosin binding protein C3, affect muscle sarcomere structure and organization such that there is loss of contractile force (Cohn et al., 2019; Wijnker et al., 2016). To use hiPSC-derived muscle in disease or toxicity models, it is therefore highly relevant to assess and quantify sarcomere length and organization, and preferably in combination with a measurement of the contractile properties.

Here, we describe an unbiased and rapid method for quantifying sarcomere length and organization in multiple muscle cell types and models, based on the SarcOmere Texture Analysis (SOTA) algorithm. SOTA was originally developed by Sutcliffe et al. (2018) to quantify sarcomere organization and length for static images in a MATLAB script. We made a user-friendly application in Python called SotaTool, which aims to enhance the performance of SOTA by implementing various background subtraction methods, adding an alignment index and including automated segmentation. In contrast to other approaches, the method does not require regions of interest (ROIs) to be pre-defined or selected, or images of fluorescent sarcomeres to be aligned manually (Cao, Manders, & Helmes, 2021; Pasqualin et al., 2016; Peterson, Kalda, & Vendelin, 2013). While current algorithms typically rely on manual user input per image to indicate the directionality of the sarcomeres, SotaTool detects the optimal angle automatically, reducing analysis time and selection bias. We show here how this software tool can be applied to many different datasets that contain sarcomeric striations: Immunostained cardiomyocytes, 3D tissue engineered skeletal muscles (3D TESMs), and phase-contrast images of primary

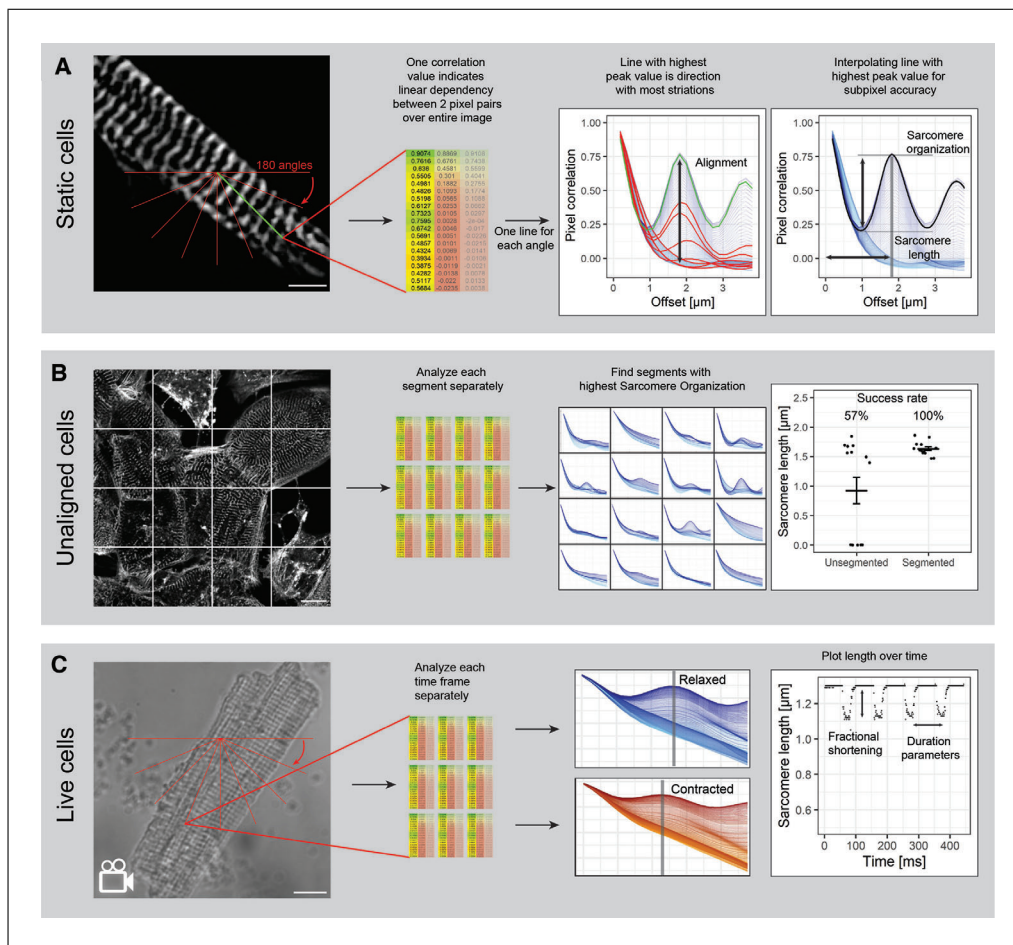


Figure 1 Broad overview of input and read-outs of the SotaTool. **(A)** SotaTool detects the correlation between pixel values at a range of offsets. This range is calculated for 180 degree angles so the algorithm can autodetect recurring patterns like striations in immunofluorescent images stained for α -actinin. For all angles the maximum is determined as sarcomere organization and the offset value of this maximum is the average sarcomere length over the entire image. Scale bar = 5 μ m. **(B)** If an image contains recurring patterns in multiple directions (e.g., in unaligned cell culture), the optimal angle to define the sarcomere length cannot be calculated properly. An optional image segmentation step resulted in a higher success rate of the sarcomere detection over 14 images of non-aligned hiPSC-CMs. Scale bar = 15 μ m. **(C)** Videos acquired from beating neonatal rat cardiomyocytes can be analyzed as single timeframes, enabling the user to find important contractile parameters: Fractional shortening, beat duration, and beat-to-beat interval. Scale bar = 10 μ m. hiPSC-CMs, human induced pluripotent stem cell-derived cardiomyocytes.

neonatal rabbit CMs. The analysis gives information on the sarcomere organization and length. Aside from static images, this tool can also be used on videos or fluorescent reporter cells, broadening the output to sarcomere shortening, contraction duration, and beat rate (Fig. 1). The approach presented here addresses several problems associated with other methods: (1) underrepresentation of the entire image available for each muscle cell, (2) tendency for selection bias, and (3) time required for analyzing large datasets.

We describe step-by-step application and validation of this protocol as a sarcomere length quantification method across multiple *in vitro* platforms, from static 2D and 3D structures in fixed tissues and cells to fractional shortening in videos of contracting muscle. We also provide step-by-step protocols for preparation and imaging of hiPSC-CM and skeletal muscle cultures that support robust analysis (Fig. 1). We expect this new tool to reduce manual labor and time necessary for multiple muscle research applications, thus facilitating discoveries on how sarcomere structure is controlled and affected by drugs and disease.

STAINING AND ANALYZING STATIC hiPSC-CMs WITH SotaTool

SotaTool is broadly applicable across multiple *in vitro* platforms in which sarcomeres are visible in contractile cells by phase contrast or fluorescent microscopy. This section describes the steps of plating, fixing, immunofluorescence staining, imaging, and analyzing 2D hiPSC-CM cultures (Fig. 2). For live cultures, the required steps are described in the next section. Here, we immunostained hiPSC-CMs for α -actinin but other sarcomeric proteins can also be stained. Better results were obtained with proteins that are part of the Z-discs or M-lines (e.g., titin, myomesin) than with A-band proteins (actin, troponin). Differentiation and immunostaining of skeletal muscle differs from the protocol described below and can be found in Iuliano et al. (2020). The acquisition and analysis (steps 29-49) are identical for all models.

Materials

- Human induced pluripotent stem cell-derived cardiomyocytes (hiPSC-CMs), either from commercial sources (e.g., Ncardia, cat. no. K0104; Fujifilm, cat. no. 11713; Axol Bio, cat. no. ax2508) or differentiated in-house using a preferred protocol
- Dulbecco's phosphate buffered saline, calcium, magnesium (DPBS; Thermo Fisher Scientific, cat. no. 14040091)
- Dulbecco's phosphate buffered saline, no calcium, no magnesium (DPBS⁻; Thermo Fisher Scientific, cat. no. 14190094)
- Multi Tissue Dissociation Kits (Miltenyi Biotec, cat. no. 130-110-204)
- BSA-based polyvinyl alcohol essential lipids (BPEL; see Ng, Davis, Stanley, & Elefanty, 2008)
- FBS (Biowest, cat. no. S00F910002)
- Matrigel Basement Membrane Matrix, LDEV-Free (Corning, cat. no. 354234)
- Paraformaldehyde (PFA; MilliporeSigma, cat. no. 158127-500G)
- Triton X-100 (MilliporeSigma, cat. no. T8787)
- Monoclonal anti- α -actinin (sarcomeric) antibody (MilliporeSigma, cat. no. A7811)
- Donkey anti-Mouse IgG (H+L) (Thermo Fisher Scientific, cat. no. a-21203)
- Tween 20 (MilliporeSigma, cat. no. P1379-100 ml)
- 4',6-Diamidino-2-phenylindole, dihydrochloride (DAPI; Thermo Fisher Scientific, cat. no. D1306)
- Immersion oil, Type-F (Leica, cat. no. 11944399)

- Personal computer (Windows or macOS) with at least 6 GB of RAM
- SP8 white light laser fluorescent confocal microscope (Leica) or equivalent, including well plate holder and 40 \times and/or higher objectives
- Centrifuge (Eppendorf, cat. no. 5810R)
- Aspirator
- 37°C humidified CO₂ cell culture incubator (Sanyo)
- Microscope for cell counting or an automated cytometer
- Falcon tube (Thermo Fisher Scientific, cat. no. 14-959-53A)
- 5-, 10-, and 25-ml sterile plastic pipets (Greiner Bio-One, cat. no. 606180, 607180, and 760180, respectively)

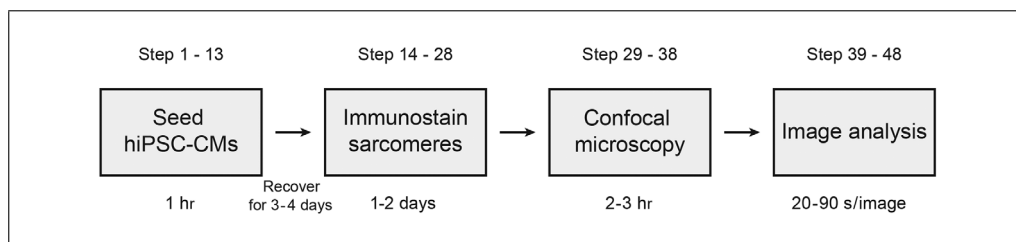


Figure 2 Strategic planning and time considerations for the protocol.

15- and 50-ml polystyrene conical tubes (Corning Falcon, cat. no. 352097 and 352098, respectively)
PIPETMAN Classic P200 and P1000 (Gilson, cat. no. F123601 and F123602, respectively)
10-, 200-, and 1,000- μ l filter tips (Corning, cat. no. 4807, 4810, and 4809, respectively)
6-well plate (Falcon, cat. no. 353046)
Falcon 96-well black/clear flat bottom microplate (Corning, cat. no. 353219)

Sample preparation

NOTE: The hiPSC-CM culture, dissociation, and replating steps are performed under aseptic conditions.

1. Thaw and culture commercially available hiPSC-CMs according to the manufacturer's instructions. Alternatively, use hiPSC-CMs differentiated using a preferred protocol (Breckwoldt et al., 2017; Correia et al., 2018; Current Protocols article: Giacomelli, Bellin, Orlova, & Mummery, 2017; Mummery et al., 2012). High (>80%) differentiation efficiency is recommended but not essential.

The protocol uses volumes recommended for 6-well plates except if stated otherwise.

2. Coat a thin-bottom 96-well plate with a 50- μ l drop of Matrigel (1:100 in DPBS for 1 hr at room temperature.

Other tissue culture grade surfaces are acceptable, although they should be appropriate for high resolution microscopy (equivalent to glass coverslips).

3. Prepare the dissociation reagent by adding 100 μ l Enzyme T to 900 μ l Buffer X from the multi tissue dissociation kit.
4. Wash cells with DPBS⁻ once (1 ml per well for 6-well plates) and aspirate.
5. Add Enzyme T/Buffer X mix to the well and incubate 10 min in a humidified incubator (37°C, 5% CO₂).

Other dissociation techniques are suitable, such as TrypLE express or collagenase. For more information, see Koc, Sahoglu Goktas, Akgul Caglar, and Cagavi (2021).

6. Add 1 ml BPEL plus 10% FBS to the well. Collect the entire volume with a P1000 pipet and mechanically disrupt the cells in suspension by gently pipetting up and down.

Critical step: Mix thoroughly but carefully. Cardiomyocytes are sensitive to mechanical stress and resuspending too harshly might decrease yield.

7. Collect all cells in a 15-ml Falcon tube.
8. Rinse the well with 2 ml BPEL plus 10% FBS and add to the Falcon tube. Repeat once.
9. Centrifuge cells at 300 \times g for 3 min and remove supernatant.
10. Add 1 ml BPEL and resuspend.
11. Count cells manually or with an automatic cytometer.
12. Add 25,000 cells to the pre-coated 96-well plate in 200 μ l BPEL.

CMs from different hiPSC lines tend to react differently to dissociation and replating. Optimization of this step (e.g., seeding density) might be necessary to reach optimal viability and morphology. We recommend that the confluency be high enough for proper cardiomyocyte morphology but not high enough to induce clumping.

13. Return to the humidified incubator and refresh BPEL after 24 hr.

Immunostaining hiPSC-CM monolayers in 96-well plates

14. After at least 3 days in culture, remove plates from the incubator and wash cells with cold DPBS⁻.

The next steps are all performed at room temperature except when stated otherwise.

15. Fix cells with 4% PFA in 0.2 M DPBS, pH 7.4 for 10 min.

CAUTION: This step must be performed in a fume hood.

16. Wash three times with DPBS⁻.
17. Permeabilize with DPBS⁻ with 0.1% Triton X-100 for 10 min.
18. Wash three times with DPBS⁻.
19. Block non-specific antibody binding for 1-2 hr with DPBS⁻ plus 10% FBS.
20. Dilute primary antibody in DPBS⁻ plus 10% FBS according to the manufacturer's instructions.
21. Remove blocking solutions and add the solution with the antibody to the cells. Incubate cells overnight at 4°C or 3 hr at room temperature.

Rocking the plate during this step can increase the penetration of the antibody and is advised.

22. Remove the antibody and wash three times with DPBS⁻ with 0.05% Tween 20 for 10 min.
23. Dilute the secondary antibody in DPBS⁻ plus 10% FBS according to the manufacturer's instructions.

Critical step: Do not expose either the antibody mix or the multi-well plate after this step to direct light.

24. Add the secondary antibody to the cells and incubate 2 hr.

Rocking the plate during this step can increase the penetration of the antibody and is advised.

25. Wash cells five times with DPBS⁻ with 0.05% Tween 20 for 5 min.
26. Counterstain with 1:500 DAPI for 10 min.

Counterstaining is not strictly necessary for the sarcomere length detection but facilitates identifying regions of interest during acquisition.

27. Wash with DPBS⁻ with 0.05% Tween 20 twice.
28. Add a volume of DPBS⁻ large enough to prevent drying.

Store the multi-well plate in a dark box or wrapped in aluminium foil to avoid exposure to light; the cells can now be stored at 4°C for several days before imaging. For optimal imaging, it is recommended that imaging be carried out <1 week after the immunostaining.

Imaging the samples

This next step can be performed on various confocal microscope systems. The Leica SP8 is given as an example.

29. Turn on the Leica SP8 confocal microscopic system, the computer, and the Leica imaging suite.

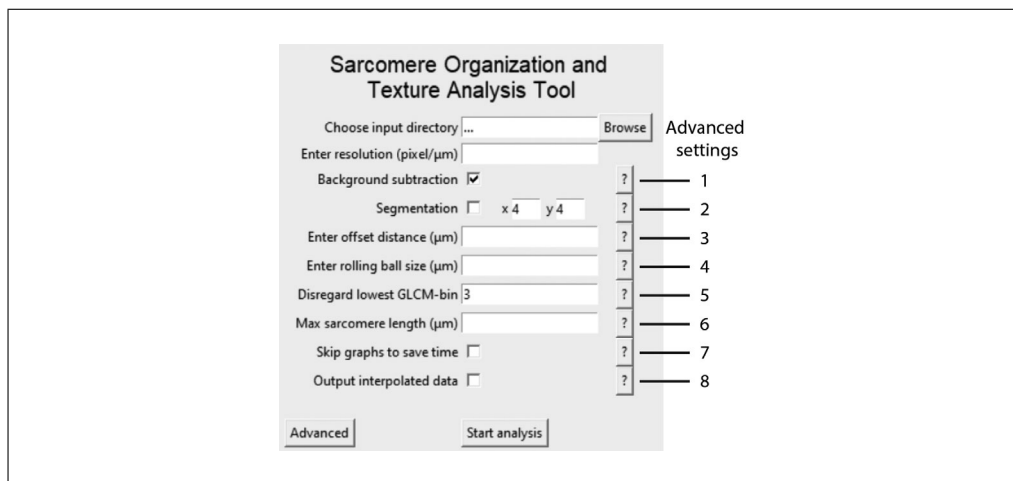


Figure 3 Graphic user interface of the SotaTool, including advanced settings. See Support Protocol 2 for details.

30. Place the 96-well plate into the appropriate holder.

31. Select the appropriate objective.

Critical step: The highest magnification will give the best spatial resolution for sarcomere length detection. An objective of at least 40× is recommended, preferably 63× and 100× lenses. For improved signal, use the appropriate immersion fluid.

32. Activate the appropriate laser light using the Leica Dye Assistant.

33. Make sure all other settings are optimal for the best resolution and minimal background.

Either frame or line averaging is recommended to reduce background fluorescence.

34. Adjust objective so that the sarcomeres are in focus.

35. Acquire at least ten to fifteen images per condition.

Critical step: Keep all microscope settings identical for all acquisitions. If settings are not kept identical, comparing different datasets or treatment conditions is impossible.

36. Export each image as a separate TIFF.

Analysis of images with the SotaTool

NOTE: The next steps can be carried out on any computer (PC) and/or laptop with sufficient hardware (see Materials list), as the SotaTool is a stand-alone application requiring no installation. Computing time will depend on the resolution, size, and bit-depth of the raw images and the PC specifications. For one 1024 × 1024 TIFF with a bit depth of 16 and the default offset of 4 μm, the computing time is ~50 s on a standard PC.

37. Transfer all TIFF images to a single folder.

Make sure the TIFF images all contain one image with sarcomeric staining (no stacks or videos).

38. Download the entire software folder of the SotaTool (www.github.com/steinjm/SotaTool) and place anywhere on the computer.

39. Double click on the executable file within the folder named SotaTool.exe.

40. Click 'Browse' to select the folder with the images to analyze (input directory, Fig. 3).

41. Input the resolution (pixels per micron).

See Support Protocol 1.

42. Press 'Start analysis'.
43. Check whether the output graphs are as expected.

See Troubleshooting (Fig. 6). A properly analyzed output graph shows a recurring sinusoid, where a vertical trendline is located at the first peak.

ALTERNATE PROTOCOL

SAMPLE PREPARATION, ACQUISITION, AND QUANTIFICATION OF FRACTIONAL SHORTENING IN LIVE REPORTER hiPSC LINES

This protocol describes the analysis of videos of hiPSC-CMs expressing a mEGFP-tagged ACTN2 protein from an ACTN2-GFP WTC hiPSC line (Roberts et al., 2019). In choosing which tagged sarcomere proteins are best to use, the same recommendations apply as for static images (see introduction of Basic Protocol). ACTN2-reporter cells were differentiated using a modified version of Giacomelli et al. (2017). Analyses of phase-contrast images or live acquisitions of neonatal rabbit cardiomyocytes using Sota-Tool are identical; a protocol for the isolation of these cells can be found in MacQuaide, Ramay, Sobie, and Smith (2010).

Additional Materials (see also Basic Protocol)

hiPSC-CMs with a mEGFP-tagged ACTN2-reporter: Allen Institute for Cell Science ACTN2-GFP WTC iPSC line (AICS-0075-085, <https://hpscereg.eu/cell-line/UCSFi001-A-4> with mEGFP inserted at ACTN2 C-terminus, obtained from Coriell Institute for Medical Research)

Andor Dragonfly 500 spinning disc inverted confocal microscope
Personal computer equipped with Andor Fusion software for microscopy and analysis (Oxford Instruments Andor, version 2.3)
On-stage incubator
Electric field stimulator (homemade or equivalent commercially available device, e.g., IonOptix myopacer cell stimulator)

Preparing the samples

The following steps are performed under aseptic conditions.

1. Perform steps 1-13 of Basic Protocol.
2. Thaw cells according manufacturer's instructions and plate on a thin-bottom 96-well plate.
3. Allow cells to recover for 24 hr and refresh medium.

Imaging the samples

NOTE: In order to extract sufficient data on the time dynamics and spatial resolution of the sarcomeric contraction, a frame rate of >50 frames per second (fps) is recommended for acquisition of live images on video. Note, this frame rate depends on the beating (and/or stimulation) frequency. For this purpose, we use an Andor Dragonfly spinning disc 500 with an on-stage incubator but an equivalent (widefield) system can be used as well.

4. Start the Andor Dragonfly spinning disc confocal system, detectors, lasers, and on-stage incubator.
5. Wait for the on-stage incubator to achieve appropriate conditions (37°C, 5% CO₂).
6. Mount the multi-well plate onto the microscope.
7. Start the Fusion software.

8. Perform steps 30-37 of Basic Protocol.

Critical step: For the laser settings, choose the 488-nm laser line for excitation. Exposure time should be kept low to achieve high fps. The histogram should have a range of at least 256 bits.

Use the appropriate immersion fluid suitable for imaging at 37°C.

9. Place the electrodes of the field stimulator in the 96-well plate and pace the cells.

Steps 9 and 10 are optional. However, we recommend imaging the cells with and without field stimulation to gain optimal insight in the contractile behavior and spontaneous beat rate.

10. Check whether the cells are “following” the imposed pacing rate.

We recommend 1.2 Hz with 5 ms duration and voltage of 15 mV bipolar pulse. If cells exhibit a fast spontaneous beat rate, higher simulation frequencies are required to avoid arrhythmic contractions. If the cells do not follow at all, increase the duration and voltage of the pulse.

11. Acquire images.

We recommend acquiring a movie consisting of at least four contractions. For example, when imaging at 50 fps and pacing at 1.2 Hz, acquire around 180 frames per position.

12. Export each image as a separate TIFF.

Ensure the timestamp is properly added to either the name or meta data of each frame. When using the Andor Dragonfly, an ImageJ macro can be found on www.github.com/steinjm/SotaTool to export all .ims-files in a folder to single TIFF files ready for analysis with SotaTool.

Extracting the fractional shortening using the SotaTool

13. Perform steps 39-47 from Basic Protocol.

14. Open the sheet with the sarcomere lengths in any preferred data visualization software (e.g., Excel, R-Studio, Graphpad).

An R-script can be found on www.github.com/steinjm/SotaTool for automated peak detection and calculation of relevant read-outs such as sarcomeric shortening, beat-beat interval, and beat duration, along with instructions for use.

15. Plot the sarcomere length on the y-axis against the timestamp on the x-axis for each separately acquired movie.

16. Note the maximum sarcomere and minimum sarcomere length and calculate the difference.

17. Divide the distance of shortening by the maximum length $\times 100\%$ for the fractional shortening of that cell.

To increase technical robustness, these last two steps can be done for each individual contraction in a movie. Using healthy cells, this fractional shortening would not differ noticeably between contractions. If this is not the case, the mean fractional shortening of all contractions should be calculated.

FINDING THE IMAGE RESOLUTION

This protocol describes the steps to determine resolution and offset distance from the image metadata.

Hardware

Personal computer (Windows or macOS) with at least 6 GB of RAM and access to the Internet

1. Download FIJI (or ImageJ) for the operating system of your computer from the following link: <https://imagej.net/software/fiji/?Downloads>.
2. Start the software.
3. Navigate to 'File' → 'Open...' and open the TIFF (or press CTR + O).
4. Navigate to 'Image' → 'Show Info' (or press CTR + I).
5. Note the resolution (pixels per micron).

If only the pixel size is found, calculate the resolution by 1/pixel size.

**SUPPORT
PROTOCOL 2****ADVANCED ANALYSIS SETTINGS**

The following section describes the settings as shown in Figure 3.

Hardware

Personal computer (Windows or macOS) with at least 6 GB of RAM and access to the Internet

1. Background subtraction greatly enhances the image quality and therefore increases accuracy of the algorithm. This is turned on by default and always recommended when no prior background subtractions have been performed on the raw data.
2. Segmentation automatically segments the original images and saves them in a subfolder for subsequent analysis.

See Support Protocol 3.

3. The offset distance is automatically defined as 4 μm but in this box the user can manually define the maximum offset distance. This greatly reduces computing time. It is crucial that the offset distance is not smaller than the expected sarcomere length.
4. Rolling ball size is automatically defined as 2 μm , which is optimized for hiPSC-CMs. Here, the user can manually override this ball size.
5. Gray-level co-occurrence matrix (GLCM)-filtering filters out the lowest gray values of the original image by disregarding the first columns and rows of the GLCM before calculating the correlation value. We have found the best default number to be three but the user can input a manual override here.

See Background Information section for more information.

6. In this box, the user can insert the maximum expected sarcomere length. This feature is useful when there is noise in the image.
7. Skip graphs to save time. We do not recommend skipping the output graphs as this is the only way to verify the analysis has been performed correctly.
8. When this box is checked, an additional .csv file is exported in the output directory with the interpolated data.

**SUPPORT
PROTOCOL 3****FINDING SARCOMERE LENGTH IN NON-ALIGNED CELLS**

The following section describes the steps needed to take multiple measurements for non-aligned cells.

Stein et al.

10 of 18

Additional Materials (also see *Basic Protocol*)

Personal computer (Windows or macOS) with at least 6 GB of RAM and access to the Internet

1. Perform Basic Protocol.
2. Check whether the program outputs values for sarcomere length or 0 values only.
3. Check the output graphs.

See Troubleshooting section.

4. If there are no peaks visible, segmentation might be necessary to find proper sarcomere length values.

See Troubleshooting section.

5. Repeat the analysis on the raw images but check ‘Segmentation’ before starting analysis.

This function will create a subfolder named ‘segments’ for saving the segments. If a new analysis is started with new segmentation settings, this folder will be emptied and new segments will be saved. Make sure there is enough free memory on the PC for the segmented images.

6. Check the output sheet. For each image, the segment with the highest sarcomere organization score has the most reliable sarcomere length but the mean of multiple (properly analyzed) segments can also be used.

COMMENTARY

Background Information

Analysis of sarcomere length of static 2D muscle cells and fractional shortening of live cells in 3D is usually time consuming, requires considerable manual labor, and is highly prone to user-selection bias. For this reason, we created a versatile, robust, and rapid method for sarcomere length quantification of many different muscle models in an open-source stand-alone Python-based application as an extension of the algorithm developed by Sutcliffe et al. (2018).

This method is based on GLCM (Haralick, Shanmugam, & Dinstein, 1973), which translates images into arrays of i columns and j rows, one for each gray level of the original image (Fig. 4A). From one GLCM, a correlation value is calculated over the entire image, which is a measure of the linear dependency for gray-value combinations over a distance g (Fig. 4B). The algorithm calculates the correlation values for 180 angles (α) over $1-g$ pixel-pixel distances (Fig. 1A).

Repeated striations in the image (such as sarcomeres) result in damped oscillating correlation graphs. To extract the direction in which the striations are most clearly present, the algorithm finds and selects the angle α at which the correlation peak is maximum. At this point, the striation-striation distance (i.e.,

the x -axis offset of the highest peak) can be determined (Fig. 1). This x -axis offset is defined as the distance g in the angle α where the highest linear dependency between gray values over the entire image is found.

By using automatic and whole-image analysis, manual labor and selection bias are decreased, because no input is required from the user except for an optional maximum micrometer offset to minimize computing time. Most importantly, the selection of areas to measure and drawing of lines for fast Fourier transformation (FFT) analysis, as done in most current practices, is not required. Most current automated analysis software is reliant on segmentation or single point tracking of the sarcomere signal, which decreases throughput or robustness in 3D stainings of sarcomeres where there is often a higher signal/noise ratio (Toepfer et al., 2019). Aside from the sarcomere length and the direction of the striations, this algorithm also outputs a measure of sarcomere organization (the maximum peak value of the correlation graphs; Sutcliffe et al., 2018) and an alignment coefficient (the variation between all the curves on the previously calculated sarcomere length; Gerbin et al., 2021). Furthermore, two other Haralick features are incorporated in the output. The uniformity (also known

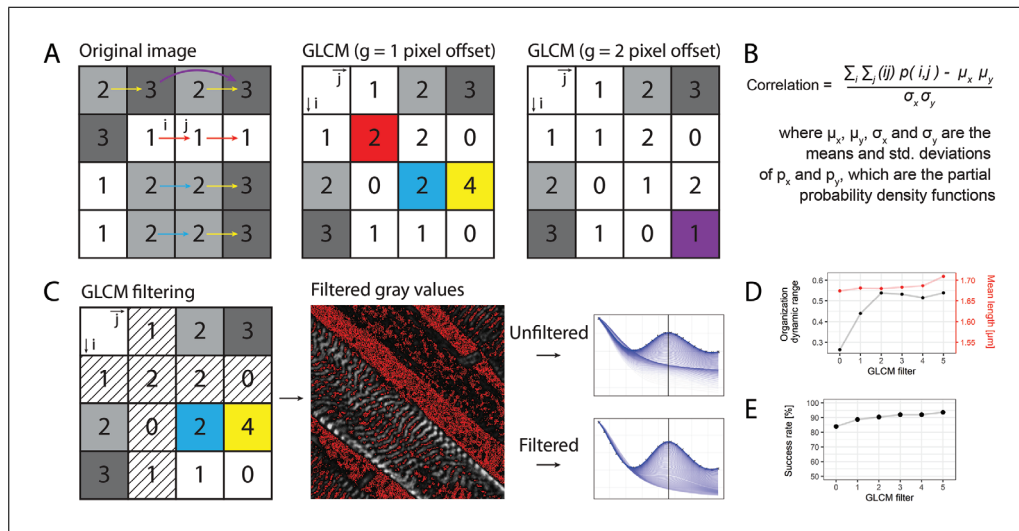


Figure 4 Visualization of the GLCM. **(A)** For each pixel in the original image, $p(ij)$ is the number of times that gray-level j occurs at a certain pixel offset g from gray-level i . **(B)** From each GLCM, a correlation feature is calculated, which results in a damped sinusoid shape when plotted against the offset if unidirectional striations are present in the image. **(C)** Filtering of the GLCM is performed before calculating the correlation values, by disregarding the first rows and first columns (the lowest bins of gray values) of the unnormalized GLCM. **(D)** This positively affects the dynamic range of the sarcomere organization score and the success rate **(E)**, but not the sarcomere length. GLCM, gray-level co-occurrence matrix.

as the angular second moment) is higher in uniform images, where 1 is a completely uniform image. The homogeneity (or the inverse difference moment) which represents image contrast, has a higher value for homogeneous images (Haralick et al., 1973; Sutcliffe et al., 2018).

One limitation of this algorithm is that images with morphologically adequate but misaligned sarcomeres do not produce correlation peaks. Therefore, we included an automated cropping step which segments the image in a user-defined manner. These segments are subsequently analyzed. In a dataset with non-aligned hiPSC-CMs cultured on standard tissue culture plastic, this increased the successful analysis of the images from 57% to 100% (see Fig. 1B). It results in a higher number of analyzed datapoints per image and requires post-processing user input to distinguish correctly from incorrectly analyzed segments. Another limitation of this method is that the metric for organization score has a narrow range, from 0 for disorganized to ~ 0.3 for organized striations. We found that disregarding the first row and first column of the GLCM (where i and j are 0) greatly reduced the background and increased the baseline sarcomere organization score, and thereby the dynamic range of the output (Fig. 4D). This method also increased the success rate of peak detection and sarcomere length calculation

in low-quality cells but did not affect the sarcomere length (Fig. 4E). It should be noted that altering the value for GLCM filtering (see Fig. 3, Advanced settings, step 5) and the value of the “rolling ball background subtraction” alters the sarcomere score and alignment but not the sarcomere length. For hiPSC-CMs, we found a filter of 3 is optimal but the user can override this in Advanced settings, step 5. To ensure broad applicability, the software does not take cell boundaries into account. Segmentation can be performed in tertiary software, such as CellProfiler (www.cellprofiler.org).

Multiple types of datasets containing striated images were analyzed and compared to other relevant methods. As shown in Figure 5, correlation of these datasets measured with SotaTool and the other methods resulted in a minimal R^2 of 0.862 among all tested datasets with p -values below .0001.

For the immunostained hiPSC-CMs cultured on micropatterned substrates (Birket et al., 2015), we performed manual length detection by creating manual line scans over the sarcomeres in ImageJ and measuring the average peak-to-peak distance. We found higher correlations between the methods and decreased absolute difference per datapoint upon increasing technical repeats of the manual detection (data not shown). This indicates that the sarcomere lengths resulting from the

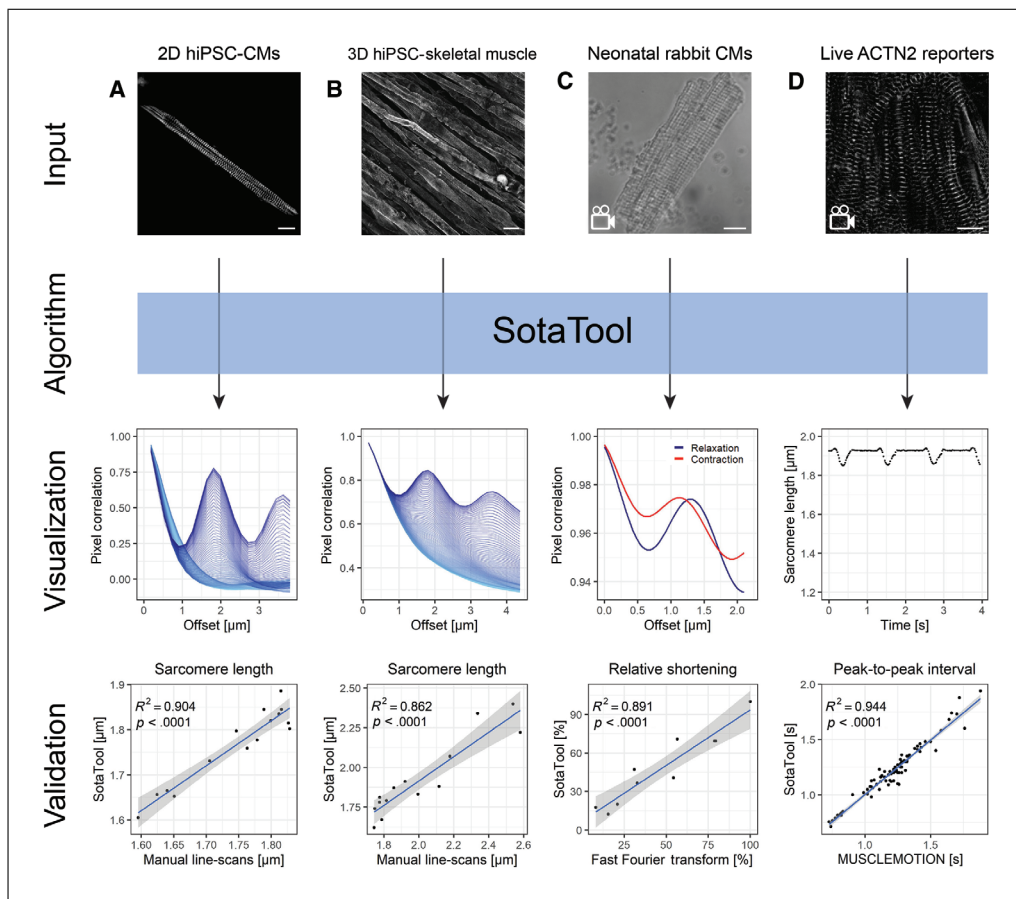


Figure 5 The SotaTool can analyze multiple types of datasets from 2D, 3D, static (fixed), and live muscle cell cultures. Datasets were analyzed with SotaTool and the gold standard for each model. Sarcomere lengths of (A) hiPSC-CMs and (B) 3D tissue engineered skeletal muscles were compared with manually determined sarcomere lengths. Linear regression shows that the results from the algorithm (y axis) correlated with the results from the manual detection method (x axis; hiPSC-CM: $p = 5.6 \times 10^{-8}$, scale bar = $15 \mu\text{m}$. hiPSC-SM: $p = 1.6 \times 10^{-6}$, scale bar = $30 \mu\text{m}$). (C) High speed phase contrast recordings of isolated neonatal rabbit cardiomyocytes were analyzed with the SotaTool. In a linear regression, the normalized fractional shortening indicated by the SotaTool correlated with the normalized fractional shortening found with fast Fourier transform ($p = 4.1 \times 10^{-5}$). Scale bar = $10 \mu\text{m}$. (D) hiPSC-CMs transduced with an mEGFP-tagged ACTN2 protein were also analyzed in a similar fashion and peak-to-peak intervals were compared to analysis with MUSCLEMOTION software ($p = 1 \times 10^{-51}$, scale bar = $10 \mu\text{m}$). hiPSC-CMs, human induced pluripotent stem cell-derived cardiomyocytes; hiPSC-SM, human induced pluripotent stem cell-derived skeletal muscle.

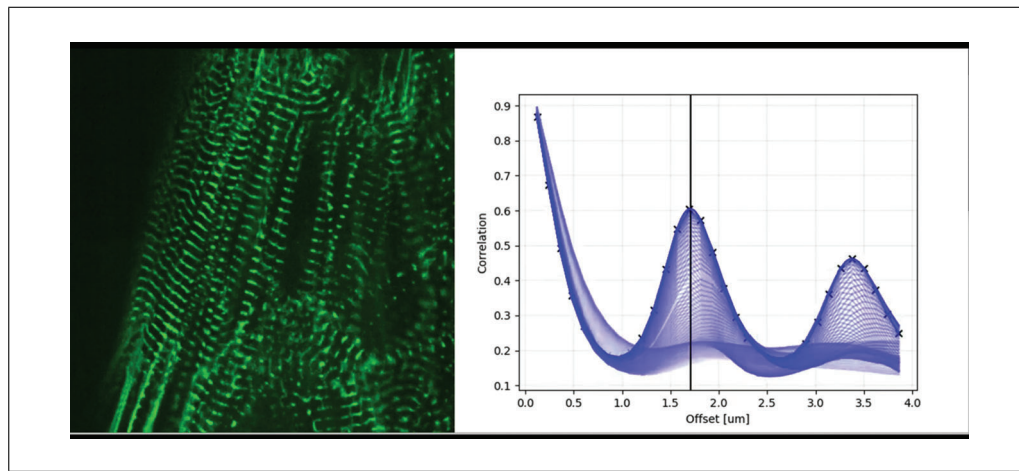
algorithm are closer to the ground truth as it takes all the striations in an entire image into account, whereas manual detection is limited by selection bias and sampling error. For the final analysis with ten manual line scans, the R^2 was 0.904 (Fig. 5A).

We applied the same method of manual detection and SotaTool analysis of images of hiPSC-derived skeletal muscle fibers cultured in 3D stained for titin. These images were chosen because the sarcomeres differ morphologically from those in hiPSC-CMs. SotaTool was able to detect striations successfully and the sarcomere length scores corresponded to those

using manual detection ($R^2 = 0.862$) taking 5 ROIs per image (Fig. 5B).

Videos of neonatal rabbit CMs with a frame rate of 100 fps were analyzed as single TIFF images (Fig. 5C). The resulting sarcomere lengths in contracted and relaxed state were subtracted, resulting in the fractional shortening. These were normalized and compared to the normalized shortening obtained using FFT analysis (Sala et al., 2018). The measurements from the two methods correlated with an R^2 of 0.891.

The live mEGFP-tagged ACTN2 reporter cells were recorded with a frame rate of



Video 1 Side-by-side view of contracting sarcomeres in hiPSC-CMs expressing ACTN2-GFP and the SotaTool output graphs. hiPSC-CMs, human induced pluripotent stem cell-derived cardiomyocytes.

50 fps and analyzed in a similar fashion and the beat rate was quantified (Fig. 5D). After SotaTool analysis of all the separate frames, the peaks were analyzed by a custom script in R-studio, which correlated with MUSCLE-MOTION ($R^2 = 0.944$; Sala et al., 2018). See Figure 8 for a representative acquisition of the reporter CMs along with the corresponding correlation graphs. Depending on the question, pacing of hiPSC-CMs might be considered. For example, the basal beat rate of hiPSC-CM can be variable between different differentiations or conditions which hampers comparison of absolute output parameters if they are not paced. On the other hand, to detect, for example, chronotropic changes, acquisition of images from spontaneously contracting cardiomyocytes are highly informative.

Analyzing live reporter cells with fluorescently tagged sarcomeres has several advantages over static cultures in which sarcomeres are immunostained. Firstly, live reporters can be monitored in real time over long periods, while immunostaining is a terminal end-point measurement. Secondly, in fixed cardiomyocytes, it is not possible to determine which cells are in systole, diastole, or an intermediate contraction/relaxation state; this may affect the sarcomere distance quantification. This is not an issue in live reporter cells where imaging is continuous. Moreover, PFA fixation can cause artefacts like cell shrinkage and disruption of cell organelles (Schnell, Dijk, Sjollem, & Giepmans, 2012). Of note though, live cell fluorescent microscopy at a high frame rate can cause phototoxicity in the cells or bleaching of the fluorescent signal and significantly more data-storage capacity

and analysis time is needed for live cell image acquisition.

Critical Parameters

A single monolayer of cells is preferred because hiPSC-CMs are easier to image and analyze than hiPSC-CMs that have formed multiple layers. This is highly dependent on seeding density but selecting the correct hiPSC-CM seeding density occasionally requires some optimization. We recommend trying different seeding densities (e.g., 16k/cm², 31k/cm², 78k/cm², 156k/cm², 234k/cm², 313k/cm², where k = × 10³) due to varying recovery efficiencies during passaging and following thawing after cryopreservation in different hiPSC-lines. Aside from the seeding density, the morphology can vary upon use of different coating proteins, e.g., Geltrex, fibronectin, or laminin instead of Matrigel.

For proper quantification of sarcomere length, the pixel size is the largest factor influencing the final result. Therefore, the images should not be “binned” during or after imaging. Moreover, an objective of over 40× is preferred for imaging. Due to the interpolation method of the algorithm, images derived using lower magnification objectives can also be analyzed to a certain extent but artefacts and incorrectly analyzed images may occur. For successful comparison of multiple datasets, the settings of the camera, laser, and SotaTool should always be identical. The same applies to the antibody dilutions and the incubation times during immunostaining.

Troubleshooting

After successful analysis, the output graph should look like Figure 6A. If there are insufficient recurring anisotropic striation patterns

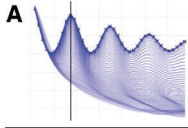
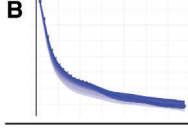
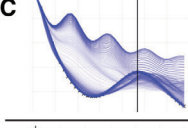
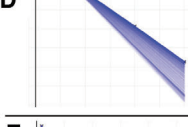
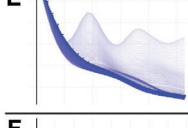
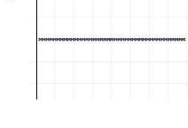
Output graph	Cause	Possible solutions
A 	Successful analysis Expected result	NA
B 	No alignment	1. Image segmentation 2. Increase GLCM threshold 3. Adjust rolling ball size
C 	Noise in image	1. Enter maximum distance 2. Decrease offset distance
D 	Entered pixel size instead of resolution	Calculate resolution and re-analyze $\text{Resolution} = 1/\text{pixel size}$
E 	Maximum sarcomere distance too low	Increase maximum distance
F 	16-bit images with wrong LUT	1. Use smaller LUT 2. Convert to 8-bit

Figure 6 Examples of good output and bad output graphs, along with troubleshooting options. Note that the numbers indicate different possible solutions and not steps to one solution. **(A)** Example of properly analyzed output image. The vertical trendline is located on the highest peak. **(B)** Result of faulty analysis due to the absence of alignment in the input image (see Support Protocol 3). **(C)** If the highest peak is not the first peak, this could indicate noise in the image. Either the offset distance or a maximum sarcomere length filter can be user defined in the advanced settings interface (step 3 and 6, respectively). **(D)** In this instance, only a small number of pixels have been analyzed, possibly because the pixel size was used instead of the resolution (i.e., pixels/ μm). **(E)** When the graph morphology is as expected but the trendline is at 0, this means the maximum sarcomere distance entered in advanced setting 6 is too low. **(F)** When the LUT of a 16-bit image has a large range (e.g., 0-65,536) but the intensity histogram is small (e.g., 100-500), this can result in all gray values of interest being in the same bin. To ensure proper analysis, these images are best pre-processed in ImageJ. Navigate to ‘Image’ → ‘Adjust’ → ‘Brightness/Contrast...’ and adjust the brightness and the contrast to the required level (LUT-range of around 255) and press ‘Apply.’ Save the image and re-run the analysis. It is crucial to choose the same range across a larger dataset. GLCM, gray-level co-occurrence matrix; LUT, look up table.

in the image, the output will look like Figure 6B. In this case, the user should opt for the automated segmentation step during analysis (see Support Protocol 3). If this still does not result in successful analysis of images, the user might use ImageJ or Photoshop to manually select an area of interest. Note that the organization parameters of manually cropped images cannot be compared to the organization of other unsegmented images. In certain cases, a recurrent noise signal can lead to output graphs like Figure 6C: Choosing maximum offset or maximum sarcomere distance

will solve this. If an output graph looks like Figure 6D, most likely the pixel size is entered instead of the resolution, which should be in pixels/ μm . If the value for the maximum sarcomere length is set too low, the output will look like 6E.

The GLCM is created by binning the original image in 256 gray values. When images with a bit depth higher than 8 are analyzed, this can result in all gray values being in the same bin (Figure 6F). These images should be pre-processed in ImageJ. Navigate to ‘Image’ → ‘Adjust’ → ‘Brightness/Contrast...’

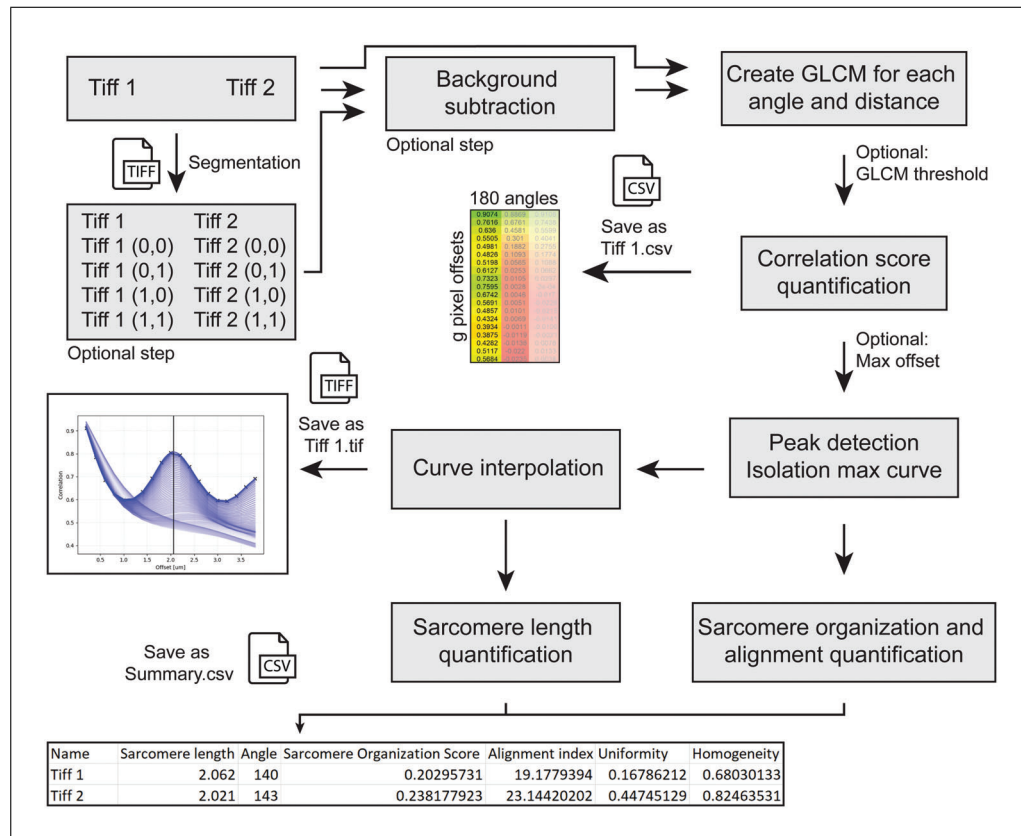


Figure 7 Flowchart of the algorithm. Optionally, single TIFF images in a folder can be segmented in a user-defined fashion and the segments are saved in a subfolder of the input directory. After optional (but defaulted) background subtraction, GLCMs are created for each angle and for g pixel offsets and 180 angles. From each GLCM a correlation value is calculated, which is saved as a table. Peak height is calculated for each angle and from the peak with the maximum value the sarcomere organization score is quantified. At this offset, the alignment index is also calculated, as the coefficient of variation of all datapoints at that offset. The selected graph with maximum organization score is interpolated for subpixel accuracy of the sarcomere length. Per image, a graph is saved with all angles, the interpolated graph and its raw datapoints, and a trendline visualizing the sarcomere length for that image. For the entire dataset, another .csv file is saved containing the file names, sarcomere lengths, angles, sarcomere organization score, and alignment

and adjust the brightness and the contrast to the required level and press “Apply”. Save the image and re-run the analysis. Preferably, the same range is chosen across a larger dataset.

If the program directly stops running without an output folder being made, this might indicate a faulty input folder, or one with restricted or password-protected access. If an output folder is made but has no content, make sure the file extension is .tif.

Understanding Results

This protocol describes an automated analysis pipeline of multiple types of data. An overview of the input, output, and algorithm steps are given in Figure 7. Broadly, after two optional pre-processing steps (background subtraction and segmentation), the GLCM is calculated, and the raw data is

saved per image as a comma delimited file (.csv). The curve with the highest peak is isolated from all the generated curves and the sarcomere organization score calculated as the difference between the height of the peak and its preceding minimum. At the offset distance of the maximum peak, the variance between all curves is taken as an alignment index. The sarcomere length is calculated from the maximum peak after interpolating with a bicubic spline, for sub-pixel accuracy. Per image, a graph is saved containing (1) all curves of all angles, (2) an overlay of the interpolated maximum graph, (3) its raw datapoints, and (4) a trendline visualizing the sarcomere length for that image. For the entire dataset, another .csv file is saved containing the file names, sarcomere lengths, angles, sarcomere organization score, and alignment

index. Optionally, the interpolated data can be saved per image as .csv (see Fig. 3, Advanced settings, step 8).

Time Considerations

For staining and analyzing static hiPSC-CMs with SotaTool, output can be generated within 5 days (Fig. 2), depending on the recovery of the cells after the thawing or seeding protocol. The immunostaining protocol includes an overnight incubation. Hands-on time during this section (Basic Protocol, steps 14 to 28) is ~1 hr for twenty wells. The second day of the immunostaining protocol is short (Basic Protocol, steps 22 to 28, <4 hr), and can be immediately followed by microscopy and data analysis. For imaging and analyzing live reporter cells, the entire experiment is shorter (~4 days, depending on the cell recovery), because no staining procedures are needed. However, data organization and analysis can take a considerable amount of time depending on the fps, resolution, size, and hardware specifications of the computer, though SotaTool can run without user supervision.

Acknowledgments

This research received support from the Netherlands Organ-on-Chip Initiative, an NWO Gravitation project funded by the Ministry of Education, Culture, and Science of the government of The Netherlands (024.003.001), from the Transnational Research Project on Cardiovascular Diseases (JTC2016_FP-40-021 ACM-HF), and from the European Research Council (ERC) under the European Union's Horizon 2020 research and innovation program (grant agreements n° 885469/ "ACQUIRE" and ERC-CoG 101001746 Mini-HEART). The Allen Cell Collection, available from Coriell Institute for Medical Research, provided materials. We thank Dr. Matthew Birket and Prof. Godfrey Smith for distribution of imaging datasets, and Prof. Dr. Jeff Saucerman for useful discussions.

Author Contributions

Jeroen M. Stein: Conceptualization, data curation, formal analysis, investigation, methodology, software, validation, visualization, writing original draft; **Ulgü Arslan:** Data curation, resources, validation; **Marnix Franken:** Data curation, resources; **Jessica C. de Greef:** Supervision, writing review and editing; **Sian E. Harding:** Resources, supervision; **Neda Mohammadi:** Data curation; **Valeria V. Orlova:** Conceptualization, funding acquisition, resources, supervision,

writing review and editing; **Milena Bellin:** Funding acquisition, supervision, writing review and editing; **Christine L. Mummery:** Funding acquisition, project administration, supervision, writing review and editing; **Berend J. van Meer:** Conceptualization, funding acquisition, methodology, resources, supervision, writing review and editing.

Conflict of Interest

C.M. is a co-founder of Ncardia BV.

Data Availability Statement

The standalone application, source code, instructions, sample images, and supporting scripts can be found on www.github.com/steinjm/SotaTool.

Literature Cited

- Birket, M. J., Ribeiro, M. C., Kosmidis, G., Ward, D., Leitoguinho, A. R., van de Pol, V., ... Mummery, C. L. (2015). Contractile defect caused by mutation in MYBPC3 revealed under conditions optimized for human PSC-cardiomyocyte function. *Cell Reports*, 13(4), 733–745. doi: 10.1016/j.celrep.2015.09.025
- Breckwoldt, K., Letuffe-Brenière, D., Mannhardt, I., Schulze, T., Ulmer, B., Werner, T., ... Hansen, A. (2017). Differentiation of cardiomyocytes and generation of human engineered heart tissue. *Nature Protocols*, 12(6), 1177–1197. doi: 10.1038/nprot.2017.033
- Cao, L., Manders, E., & Helmes, M. (2021). Automatic detection of adult cardiomyocyte for high throughput measurements of calcium and contractility. *PLoS One*, 16(9), e0256713. doi: 10.1371/journal.pone.0256713
- Cohn, R., Thakar, K., Lowe, A., Ladha, F. A., Petinato, A. M., Romano, R., ... Hinson, J. T. (2019). A contraction stress model of hypertrophic cardiomyopathy due to sarcomere mutations. *Stem Cell Reports*, 12(1), 71–83. doi: 10.1016/j.stemcr.2018.11.015
- Correia, C., Koshkin, A., Duarte, P., Hu, D., Carido, M., Sebastião, M. J., ... Serra, M. (2018). 3D aggregate culture improves metabolic maturation of human pluripotent stem cell derived cardiomyocytes. *Biotechnology and Bioengineering*, 115(3), 630–644. doi: 10.1002/bit.26504
- Gerbin, K. A., Grancharova, T., Donovan-Maiye, R. M., Hendershott, M. C., Anderson, H. G., Brown, J. M., ... Gunawardane, R. N. (2021). Cell states beyond transcriptomics: Integrating structural organization and gene expression in hiPSC-derived cardiomyocytes. *Cell Systems*, 12(6), 670–687.e10. doi: 10.1016/j.cels.2021.05.001
- Giacomelli, E., Bellin, M., Orlova, V. V., & Mummery, C. L. (2017). Co-differentiation of human pluripotent stem cells-derived cardiomyocytes and endothelial cells from cardiac mesoderm provides a three-dimensional model of cardiac microtissue. *Current Protocols in*

- Human Genetics*, 95(1), 21.9.1–21.9.22. doi: 10.1002/cphg.46
- Giacomelli, E., Meraviglia, V., Campostrini, G., Cochrane, A., Cao, X., van Helden, R. W. J., ... Mummery, C. L. (2020). Human-iPSC-derived cardiac stromal cells enhance maturation in 3D cardiac microtissues and reveal non-cardiomyocyte contributions to heart disease. *Cell Stem Cell*, 26(6), 862–879.e11. doi: 10.1016/j.stem.2020.05.004
- Haralick, R. M., Shanmugam, K., & Dinstein, I. (1973). Textural features for image classification. *IEEE Transactions on Systems, Man, and Cybernetics, SMC-3*(6), 610–621. doi: 10.1109/TSMC.1973.4309314
- Iuliano, A., Wal, E., Ruijmbek, C. W. B., in 't Groen, S. L. M., Pijnappel, W. W. M. P., Greef, J. C., & Saggiomo, V. (2020). Coupling 3D printing and novel replica molding for in house fabrication of skeletal muscle tissue engineering devices. *Advanced Materials Technologies*, 5, 2000344. doi: 10.1002/admt.202000344
- Jalal, S., Dastidar, S., & Tedesco, F. S. (2021). Advanced models of human skeletal muscle differentiation, development and disease: Three-dimensional cultures, organoids and beyond. *Current Opinion in Cell Biology*, 73(August), 92–104. doi: 10.1016/jceb.2021.06.004
- Koc, A., Sahoglu Goktas, S., Akgul Caglar, T., & Cagavi, E. (2021). Defining optimal enzyme and matrix combination for replating of human induced pluripotent stem cell-derived cardiomyocytes at different levels of maturity. *Experimental Cell Research*, 403(2), 112599. doi: 10.1016/j.yexcr.2021.112599
- MacQuaide, N., Ramay, H. R., Sobie, E. A., & Smith, G. L. (2010). Differential sensitivity of Ca²⁺ wave and Ca²⁺ spark events to ruthenium red in isolated permeabilised rabbit cardiomyocytes. *The Journal of Physiology*, 588(23), 4731–4742. doi: 10.1113/jphysiol.2010.193375
- Mills, R. J., Titmarsh, D. M., Koenig, X., Parker, B. L., Ryall, J. G., Quaipe-Ryan, G. A., ... Hudson, J. E. (2017). Functional screening in human cardiac organoids reveals a metabolic mechanism for cardiomyocyte cell cycle arrest. *Proceedings of the National Academy of Sciences*, 114(40), E8372–E8381. doi: 10.1073/pnas.1707316114
- Mummery, C. L., Zhang, J., Ng, E. S., Elliott, D. A., Elefanty, A. G., & Kamp, T. J. (2012). Differentiation of human embryonic stem cells and induced pluripotent stem cells to cardiomyocytes. *Circulation Research*, 111(3), 344–358. doi: 10.1161/CIRCRESAHA.110.227512
- Ng, E. S., Davis, R., Stanley, E. G., & Elefanty, A. G. (2008). A protocol describing the use of a recombinant protein-based, animal product-free medium (APEL) for human embryonic stem cell differentiation as spin embryoid bodies. *Nature Protocols*, 3(5), 768–776. doi: 10.1038/nprot.2008.42
- Pasqualin, C., Gannier, F., Yu, A., Malécot, C. O., Bredeloux, P., & Maupoil, V. (2016). SarcOptiM for ImageJ: High-frequency online sarcomere length computing on stimulated cardiomyocytes. *American Journal of Physiology-Cell Physiology*, 311(2), C277–C283. doi: 10.1152/ajpcell.00094.2016
- Peterson, P., Kalda, M., & Vendelin, M. (2013). Real-time determination of sarcomere length of a single cardiomyocyte during contraction. *American Journal of Physiology-Cell Physiology*, 304(6), C519–C531. doi: 10.1152/ajpcell.00032.2012
- Ribeiro, M. C., Tertoolen, L. G., Guadix, J. A., Bellin, M., Kosmidis, G., D'Aniello, C., ... Passier, R. (2015). Functional maturation of human pluripotent stem cell derived cardiomyocytes *in vitro* – Correlation between contraction force and electrophysiology. *Biomaterials*, 51, 138–150. doi: 10.1016/j.biomaterials.2015.01.067
- Roberts, B., Hendershott, M. C., Arakaki, J., Gerbin, K. A., Malik, H., Nelson, A., ... Gunawardane, R. N. (2019). Fluorescent gene tagging of transcriptionally silent genes in hiPSCs. *Stem Cell Reports*, 12(5), 1145–1158. doi: 10.1016/j.stemcr.2019.03.001
- Sala, L., van Meer, B. J., Tertoolen, L. G. J., Bakkers, J., Bellin, M., Davis, R. P., ... Mummery, C. L. (2018). Musclemotion. *Circulation Research*, 122(3), e5–e16. doi: 10.1161/CIRCRESAHA.117.312067
- Schnell, U., Dijk, F., Sjollem, K. A., & Giepmans, B. N. G. (2012). Immunolabeling artifacts and the need for live-cell imaging. *Nature Methods*, 9(2), 152–158. doi: 10.1038/nmeth.1855
- Sutcliffe, M. D., Tan, P. M., Fernandez-Perez, A., Nam, Y.-J., Munshi, N. V., & Saucerman, J. J. (2018). High content analysis identifies unique morphological features of reprogrammed cardiomyocytes. *Scientific Reports*, 8(1), 1258. doi: 10.1038/s41598-018-19539-z
- Toepfer, C. N., Sharma, A., Cicconet, M., Garfinkel, A. C., Mücke, M., Neyazi, M., ... Seidman, C. E. (2019). SarcTrack: An adaptable software tool for efficient large-scale analysis of sarcomere function in hiPSC-Cardiomyocytes. *Circulation Research*, 124(8), 1172–1183. doi: 10.1161/CIRCRESAHA.118.314505
- van der Velden, J., Klein, L. J., van der Bijl, M. J. A. M., Huybregts, M. A., Stoker, W., Witkop, J., ... Stienen, G. J. M. (1998). Force production in mechanically isolated cardiac myocytes from human ventricular muscle tissue. *Cardiovascular Research*, 38(2), 414–423. doi: 10.1016/S0008-6363(98)00019-4
- Wijnker, P. J. M., Friedrich, F. W., Dutsch, A., Reischmann, S., Eder, A., Mannhardt, I., ... Carrier, L. (2016). Comparison of the effects of a truncating and a missense MYBPC3 mutation on contractile parameters of engineered heart tissue. *Journal of Molecular and Cellular Cardiology*, 97, 82–92. doi: 10.1016/j.yjmcc.2016.03.003
- Yang, X., Pabon, L., & Murry, C. E. (2014). Engineering adolescence: Maturation of human pluripotent stem cell-derived cardiomyocytes. *Circulation Research*, 114(3), 511–523. doi: 10.1161/CIRCRESAHA.114.300558